[1] *Synth. Met.* **1997**, 84–86 (*Proc.* ICSM (Snowbird, UT), **1996**).
[2] a) J. M. Williams, A. J. Schultz, U. Ceiser, K. D. Carlson, A. M. Kini, H. H. Wang, W.-K. Kwok, M.-H. Whangbo, J. E. Schirber, *Science* **1991**, *252*, 1501–1508; b) J. M. Williams, J. R. Ferraro, R. J. Thorn, K. D. Carlson, U. Geiser, H. H. Wang, A. M. Kini, M.-H. Whangbo, *Organic Superconductors (Including Fullerenes)*, Prentice Hall, Englewood Cliffs, NJ, **1992**.
[3] Structural isomers of BEDT-TTF have been reported recently: a) P. Hudhomme, P. Blanchard, M. Sallé, S. Le Moustarder, A. Riou, M. Jubault, A. Gorgues, G. Duguay, *Angew. Chem.* **1997**, *109*, 896–899; *Angew. Chem. Int. Ed. Engl.* **1997**, *36*, 878–881; b) C. Durand, P. Hudhomme, G. Duguay, M. Jubault, A. Gorgues, *Chem. Commun.* **1998**, 361–362.
[4] a) J. Yamada, S. Takasaki, M. Kobayashi, H. Anzai, N. Tajima, M. Tamura, Y. Nishio, K. Kajita, *Chem. Lett.* **1995**, 1069–1070; b) J. Yamada, S. Mishima, H. Anzai, M. Tamura, Y. Nishio, K. Kajita, T. Sato, H. Nishikawa, I. Ikemoto, K. Kikuchi, *Chem. Commun.* **1996**, 2517–2518.
[5] J. Yamada, R. Oka, H. Anzai, H. Nishikawa, I. Ikemoto, K. Kikuchi, *Tetrahedron Lett.* **1998**, *39*, 7709–7712.
[6] a) J. Yamada, Y. Amano, S. Takasaki, R. Nakanishi, K. Matsumoto, S. Satoki, H. Anzai, *J. Am. Chem. Soc.* **1995**, *117*, 1149–1150; b) J. Yamada, S. Satoki, S. Mishima, N. Akashi, K. Takahashi, N. Masuda, Y. Nishimoto, S. Takasaki, H. Anzai, *J. Org. Chem.* **1996**, *61*, 3987–3995.
[7] H. Kobayashi, A. Kobayashi, Y. Sasaki, G. Saito, H. Inokuchi, *Bull. Chem. Soc. Jpn.* **1986**, *59*, 301–302.
[8] H. Anzai, J. M. Delrieu, S. Takasaki, S. Nakatsuji, J. Yamada, *J. Cryst. Growth* **1995**, *154*, 145–150.
[9] H. Urayama, H. Yamachi, G. Saito, S. Sato, A. Kawamoto, J. Tanaka, T. Mori, Y. Maruyama, H. Inokuchi, *Chem. Lett.* **1988**, 463–466.
[10] Y. Misaki, N. Higuchi, T. Ohta, H. Fujiwara, T. Yamabe, T. Mori, H. Mori, S. Tanaka, *Mol. Cryst. Liq. Cryst.* **1996**, *284*, 27–38.
[11] For non-TTF donors which are designed to form 2D stacks, see, for example, K. Takimiya, Y. Shibata, A. Ohnishi, Y. Aso, T. Otsubo, F. Ogura, *J. Mater. Chem.* **1995**, *5*, 1539–1547, and references therein.

$[\{MeAl(\mu_2\text{-}F)\}_2N(2,6\text{-}i Pr_2C_6H_3)]_4$—A Molecular Al-F-N Cage Compound**

Helge Wessel, Hyung-Suh Park, Peter Müller, Herbert W. Roesky,* and Isabel Usón

AlN and AlF_3 are high-melting, temperature-stable solids that are insoluble in organic solvents. In the last years soluble precursors of both compounds have become available which lead to AlN[1] and AlF_3[2], respectively, upon elimination under relatively mild conditions. Our goal now was to find out whether it is possible to combine the two systems and to synthesize soluble precursors containing Al, F, and N. Here we describe the synthesis of $[(2,6\text{-}iPr_2C_6H_3NH)MeAl(\mu_2\text{-}F)]_4$ (**1**) and its pyrolysis to the first Al-F-N cage compound **2**, which was characterized by X-ray structure analysis,[3] NMR and IR spectroscopy as well as mass spectrometry. Compound **2** was obtained as colorless crystals after a two-step elimination reaction from Me_2AlF and $(2,6\text{-}iPr_2C_6H_3)NH_2$ (Scheme 1).

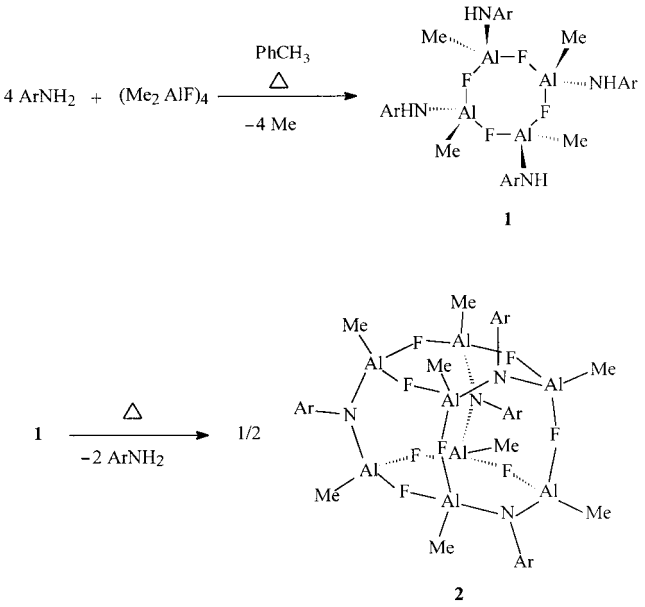

Scheme 1. Synthesis of **1** and **2**. Ar = 2,6-$iPr_2C_6H_3$.

In the first step of the reaction, one methyl group at each Al atom of the eight-membered starting material $(Me_2AlF)_4$[4] was replaced by a $(2,6\text{-}iPr_2C_6H_3)NH$ residue under methane elimination. Compound **1** was isolated and characterized: In the EI mass spectrum the peak for $[M-3Me]^+$ was detected at m/z 902, the ^{19}F NMR signals ($\delta = -141$ and -140) for the Al-bridging fluorine atoms were in accord with those of known Al-F-Al substructures,[5, 6] and the elemental analysis confirmed the composition. The pyrolysis of **1** then surprisingly took place under $(2,6\text{-}iPr_2C_6H_3)NH_2$ elimination. This reaction sequence, which takes place at two very different temperatures, allowed the isolation of **2** in high yields.

Compound **2** crystallizes in the tetragonal space group $P\bar{4}2_1c$ with one-quarter of a molecule in the asymmetric unit; the remaining three-quarters are generated by the $\bar{4}$ axis. The center of the structure is a cubic cage, the six faces of which form four eight-membered $Al_4N(\mu_2\text{-}F)_3$ rings in a half-chair conformation and two likewise eight-membered $Al_4N_2(\mu_2\text{-}F)_2$ rings in a boat conformation (Figure 1). All rings consist of alternating metal and nonmetal atoms. To complete the coordination sphere each Al atom carries a methyl group, and each N atom is bound to a 2,6-diisopropylphenyl residue.

The mean Al–N bond length in **2** (1.788(3) Å) lies within the typical range for Al–N bonds,[7] the Al–F bonds (on average 1.785(3) Å) are longer than Al–F single bonds (1.65 Å), but quite typical for μ_2-bridging F atoms.[8] The aluminum atoms are all coordinated in a slightly distorted tetrahedron (angular sum 651.5° (ideal tetrahedron: 657.0°)), in which four groups of angles can be distinguished: F-Al-F (1 ×), C-Al-N (1 ×), N-Al-F (2 ×), and C-Al-F angles (2 ×).

[*] Prof. Dr. H. W. Roesky, Dipl.-Chem. H. Wessel, Dr. H.-S. Park, Dipl.-Chem. P. Müller, Dr. I. Usón
Institut für Anorganische Chemie der Universität
Tammannstrasse 4, D-37077 Göttingen (Germany)
Fax: (+49) 551-39-3373
E-mail: hroesky@gwdg.de

[**] This work was supported by the Deutsche Forschungsgemeinschaft, the Bundesministerium für Bildung, Forschung und Technologie, the Witco GmbH, Bergkamen, and the Göttinger Akademie der Wissenschaften. H.W. thanks the Fonds der Chemischen Industrie for a doctoral fellowship.

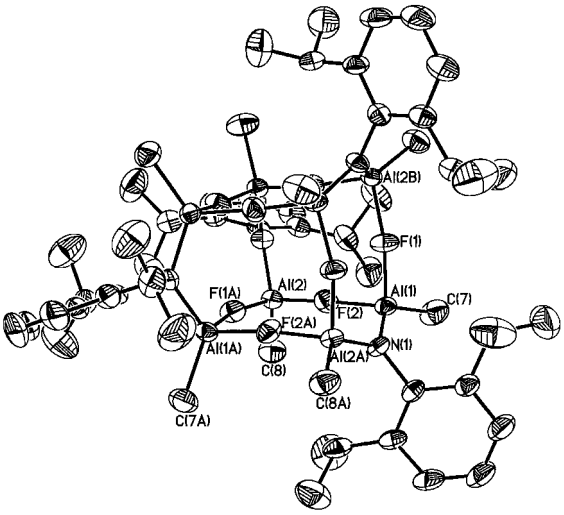

Figure 1. Molecular structure of **2** in the crystal. Selected distances [Å] and angles [°]: Al(1)–F(2) 1.776(3), Al(1)–N(1) 1.793 (3), Al(2)–F(2) 1.792(3), Al(1)–F(1) 1.784(2), Al(2)–C(8) 1.918(4); F(2)-Al(1)-F(1) 92.6(1), F(1)-Al(1)-N(1) 107.5(1), F(1)-Al(1)-C(7) 109.6(2), F(2)-Al(1)-N(1) 107.0(1), Al(1)-F(1)-Al(2B) 164.4(2), Al(1)-F(2)-Al(2) 173.3(2), Al(1)-N(1)-Al(2A) 125.9(2).

The F-Al-F angles are smaller than the ideal tetrahedral angle of 109.5° (on average 91.9(1)°), the C-Al-N angles are larger (on average 126.2(2)°), and the N-Al-F and C-Al-F angles (on average 107.1(1) and 109.6(2)°, respectively) are very close to the ideal tetrahedral angle. The nitrogen atoms in the eight-membered rings have a planar environment within the experimental error: The angular sum around them amounts to 359.8(2)°; the mean deviation from the best plane is 0.003 Å. The two Al-N-Al angles are equal for reasons of symmetry and amount to 125.9(2)°. The two independent Al-F-Al angles differ significantly: If the bridging fluorine atom belongs to an $Al_4N_2F_2$ ring, the angle is 164.4(2)° (Al(1)-F(1)-Al(2B)), if it belongs to an Al_4NF_3 ring, 173.3(2)° (Al(1)-F(2)-Al(2)).

Compound **2** can be considered as an entry into a new class of compounds and can draw a varied chemistry with it due to its reactive substituents. For its use in metal organic chemical vapor deposition (MOCVD) methods the system has to be modified in future work in such a way that good leaving groups are introduced as substituents in order to prevent the deposition of carbon.

Experimental Section

1: Me_2AlF (20 mL of a 2.5 M solution in toluene) was added dropwise to a solution of (2,6-*i*$Pr_2C_6H_3$)NH_2 (9.41 mL, 50.0 mmol) in toluene (75 mL) at room temperature. Subsequently the reaction mixture was heated for 10 h under reflux, during which time the evolving methane was led off through a mercury pressure relief valve. After all volatile components were removed in vacuo, the residue was washed with *n*-hexane (30 mL), and **1** was obtained as a white solid (40.3 g, 85 %). M.p. 152 °C; ^{1}H NMR (200 MHz, C_6D_6, TMS): $\delta = -0.22$ (m, 12 H, $AlCH_3$), 1.15 (m, 48 H, $CH(CH_3)_2$), 3.35 (m, 8 H, $CH(CH_3)_2$), 3.85 (s, 2 H, NH), 4.05 (s, 2 H, NH), 6.95 (m, 12 H, arom. H); ^{19}F NMR (235 MHz, C_6D_6, $CFCl_3$): $\delta = -141$ (s, 2 F), -140 (s, 2 F); IR (KBr, nujol): $\tilde{\nu}$ = 3369, 3258, 1621, 1592, 1433, 1379, 1343, 1309, 1255, 1211, 1168, 1100, 1043, 976, 887, 866, 820, 762, 705, 670, 570, 545, 427 cm^{-1}; MS (EI): *m*/*z* (%): 902 (2, $M-3$Me), 162 (100, $C_{12}H_{18}$); elemental analysis calcd for $C_{52}H_{84}Al_4F_4N_4$: C 65.8, H 8.9, Al 11.4, N 5.9; found: C 65.7, H 9.2, Al 11.1, N 6.2.

2: Compound **1** (4.7 g, 5.0 mmol) was heated to 165 °C for 3 h. The crude product was then washed with *n*-hexane (15 mL), and **2** was obtained as a white microcrystalline solid (3.8 g, 80 %). Single crystals were grown from *n*-hexane at -22 °C within two months. M.p. 180 °C; ^{1}H NMR (200 MHz, C_6D_6, TMS): $\delta = -0.31$ (m, 24 H, $AlCH_3$), 1.51 (m, 48 H, $CH(CH_3)_2$), 3.40 (sept., 8 H, $CH(CH_3)_2$), 6.95 (m, 12 H, arom. H); ^{19}F NMR (235 MHz, C_6D_6, $CFCl_3$): $\delta = -144$ to -140 (4 s, 8 F);[6] IR (KBr, nujol): $\tilde{\nu}$ = 1943, 1608, 1577, 1539, 1509, 1419, 1348, 1260, 1168, 1089, 1077, 1039, 1023, 864, 833, 801, 740, 722, 565 cm^{-1}; MS (EI): *m*/*z* (%): 581 (2, $M/2-$Me), 162 (100, $C_{12}H_{18}$); elemental analysis calcd for $C_{56}H_{92}Al_8F_8N_4$: C 56.6, H 7.7, F 12.8, N 4.7; found: C 57.0, H 7.6, F 12.4, N 4.7.

Received: October 19, 1998 [Z 12537IE]
German version: *Angew. Chem.* **1999**, *111*, 850–852

Keywords: aluminum · aminoalanes · cage compounds · fluorine

[1] a) W. Rockensüss, H. W. Roesky, *Adv. Mater.* **1993**, *5*, 443; b) Z. P. Jiang, L. V. Interrante, *Chem. Mater.* **1990**, *2*, 439; c) A. C. Jones, *J. Cryst. Growth* **1993**, *129*, 728; K. L. Ho, K. F. Jansen, J. W. Hwang, W. L. Gladfelter, J. F. Evans, *J. Cryst. Growth* **1991**, *107*, 376; d) D. A. Neumayer, J. G. Erkerd, *Chem. Mater.* **1996**, *8*, 9.

[2] a) A. Le Bail, J. L. Fourquet, *J. Solid State Chem.* **1992**, *100*, 151; b) N. Herron, D. L. Thorn, R. L. Harlow, G. A. Jones, J. B. Parise, J. A. Fernandez-Baca, T. Vogt, *Chem. Mater.* **1995**, *7*, 75.

[3] Crystal data for **2**: $C_{56}H_{92}Al_8F_8N_4$, M_r = 1189.18, crystal dimensions: 0.40 × 0.40 × 0.10 mm, tetragonal, $P\bar{4}2_1c$, a = 12.751(2), c = 21.058(4) Å, V = 3424(1) Å^3, ρ_{calcd} = 1.153 g cm^{-3}, Z = 2, absorption coefficient μ = 0.177 mm^{-1}, maximal resolution 2θ = 46.5°; of 36 517 measured reflections, 2466 were independent (R_{int} = 0.1982). Ratio data:restraints:parameters 2466:0:178, final R values: $R1$ = 0.0462, $wR2$ = 0.1087 for data with $I > 2\sigma(I)$, $R1$ = 0.0788, $wR2$ = 0.1217 for all data, goodness of fit S = 0.962; ($R1 = \Sigma\,||F_o|-|F_c||/\Sigma\,|F_o|$, $wR2 = \Sigma w(F_o^2 - F_c^2)^2/\Sigma w(F_o^2)^2]^{1/2}$, $S = [\Sigma w(F_o^2 - F_c^2)^2\,/\Sigma(n-p)]^{1/2}$); weighting scheme: $w^{-1} = \Sigma^2(F_o)^2 + (0.0784\ \ P)^2 + 0.000\,P$; $P = [F_o^2 + 2F_c^2]/3$; greatest residual electron density/sink 0.222/$-$0.272 e A^{-3}. The choice of enantiomer was made based on the Flack x parameter: For the chosen enantiomer this parameter amounted to -0.36 with a standard deviation of 0.3, for the inverted structure 1.37 with the same standard deviation. The better R value of the described enantiomer also supports this choice. The crystal was removed from the Schlenck flask under protective gas, mounted on a glass thread with perfluoropolyether, and quickly frozen.[9] The data were collected at 133 K on a Stoe-Siemens-Huber four-circle diffractometer with a Siemens-CCD area detector with graphite-monochromatized $Mo_{K\alpha}$ radiation (λ = 0.71073 Å); the intensities were recorded with φ and ω scans. The structure was solved with direct methods (program SHELXS-97)[10] and refined against F^2 with the full-matrix least-squares method using the program SHELXL-97.[11] All non-hydrogen atoms were refined anisotropically, and the hydrogen atoms were added to geometrically calculated positions and refined with a riding model. Crystallographic data (excluding structure factors) for the structure reported in this paper have been deposited with the Cambridge Crystallographic Data Centre as supplementary publication no. CCDC-103311. Copies of the data can be obtained free of charge on application to CCDC, 12 Union Road, Cambridge CB2 1EZ, UK (fax: (+44) 1223-336-033; e-mail: deposit@ccdc.cam.ac.uk).

[4] a) G. Gunderson, T. Haugen, A. Haaland, *J. Organomet. Chem.* **1973**, *54*, 77; b) J. Weidlein, V. Krieg, *J. Organomet. Chem.* **1968**, *11*, 9.

[5] a) S. D. Waezsada, F.-Q. Liu, E. F. Murphy, H. W. Roesky, M. Teichert, I. Usón, H.-G. Schmidt, T. Albers, E. Parisini, M. Noltemeyer, *Organometallics* **1997**, *16*, 1260; b) H. Wessel, M. L. Montero, C. Rennekamp, H. W. Roesky, P. Yu, I. Usón, *Angew. Chem.* **1998**, *110*, 862; *Angew. Chem. Int. Ed.* **1998**, *37*, 843.

[6] The ^{19}F NMR spectra of **1** and **2** always showed the same number of resonance lines in the temperature range from -60 to $+60$ °C in toluene/C_6D_6 (10/1). This speaks for an Al_4F_4 ring in **1** which, due to the steric requirements of the ligands, is not planar or for a dissociation of **1** and **2** in solution into smaller structure units.

  1433-7851/99/3806-0814 $ 17.50+.50/0

[7] R. J. Wehmschulte, P. P. Power, *J. Am. Chem. Soc.* **1996**, *118*, 791.
[8] a) N. E. Brese, M. O'Keefe, *Acta Crystallogr. Sect. B* **1991**, *47*, 192; b) S. D. Waezsada, F.-Q. Liu, C. E. Barnes, H. W. Roesky, M. L. Montero, I. Usŏn, *Angew. Chem.* **1997**, *109*, 2738; *Angew. Chem. Int. Ed. Engl.* **1997**, *36*, 2625.
[9] T. Kottke, D. Stalke, *J. Appl. Crystallogr.* **1993**, *26*, 615.
[10] G. M. Sheldrick, *Acta Crystallogr. Sect. A* **1990**, *46*, 467.
[11] G. M. Sheldrick, SHELX 97, Universität Göttingen, Germany, **1997**.

Energetics of Molecular Complexes in a Supersonic Beam: A Novel Spectroscopic Tool for Enantiomeric Discrimination**

Andrea Latini, Daniela Toja, Anna Giardini-Guidoni, Susanna Piccirillo, and Maurizio Speranza*

Enantiomeric discrimination takes place when a chiral selector (C) forms with a pair of enantiomers (M) two diastereomeric molecular complexes (MCs) of different stability (thermodynamic enantioselectivity). This is the basis of chiral chromatography, enzymic resolution, asymmetric synthesis, and NMR spectroscopic discrimination with chiral auxiliaries.[1, 2] Although the principles of thermodynamic enantioselectivity find eminent applications in many fields, very few experiments have been designed so far to establish at the microscopic level the nature and energetics of the various interactions in diastereomeric MCs.

Thermometric measurements of the energetics of aggregation of chiral ions in solution to make diastereomeric ion pairs were first carried out by Arnett and Zingg.[3] These authors pointed out that the average difference in thermodynamic stability between diastereomeric combinations of several chiral amines with mandelic acid enantiomers may span from zero to $200-350\ \mathrm{cal\,mol^{-1}}$, depending upon the structure of the amine and the nature of the solvent.

A way to evaluate the intrinsic nature of the various interactions in diastereomeric MCs and to eliminate the moderating effects of solvent on their energetics is to study their features in the isolated state. Here we report on the first spectroscopic determination of the binding energy in isolated diastereomeric MCs, with special regard to the dependence of the binding energy on the configuration of the chiral solvent molecule.

Weakly bound MCs, which would be unobservable at room temperature, can be readily generated in the isolated state by supersonic expansion of their components. Under these conditions, they are formed at an average temperature of a few Kelvins[4] and can be spectroscopically discriminated. The spectral analysis is facilitated by the fact that, at low temperatures, only the lowest rotational and vibrational levels are populated. Lahmani and co-workers recently characterized jet-cooled diastereomeric MCs by different laser-induced fluorescence (LIF) spectra.[5–7] Discrimination between diastereomeric MCs was obtained by us[8] with resonance-enhanced multiphoton ionization (REMPI) spectroscopy combined with time-of-flight (TOF) mass spectrometry.[4, 9] Accordingly, the REMPI-TOF spectra of the diastereomeric molecular complexes **Rr** and **Rs**—formed from the combination of the chiral chromophore (*R*)-(+)-1-phenyl-1-propanol (**R**) with (*R*)-(−) (**r**) and (*S*)-(+)-2-butanol (**s**), respectively—display different features. In particular, their most intense band, assigned to the electronic band origin, is red-shifted relative to the $S_1 \leftarrow S_0$ band origin of the isolated **R** molecule ($\Delta\nu = -79\ \mathrm{cm^{-1}}$ (**Rr**), $-92\ \mathrm{cm^{-1}}$ (**Rs**)), indicating an enhancement of binding energy of both **Rr** and **Rs** adducts in the S_1 state relative to the S_0 state. The difference between the red shifts ($\Delta\nu[\mathbf{Rr}] - \Delta\nu[\mathbf{Rs}] = 13\ \mathrm{cm^{-1}}$) reflects a $S_1 \leftarrow S_0$ energy gap for **Rs** which is smaller than for **Rr**.

The binding energy of the diastereomeric **Rr** and **Rs** adducts was measured by two color resonance two photon ionization (2cR2PI) experiments. The species under investigation is selectively excited to the S_1 state by absorption of one photon at a fixed frequency ν_1 ($h\nu_1$ in Figure 1), and then ionized by a second photon of variable frequency ν_2 ($h\nu_2$ in Figure 1). The experimental procedure is the following: the species under unvestigation was first submitted to one color resonance two photon ionization (1cR2PI) experiments,[8] in which it is excited to a discrete S_1 state by absorption of one photon of frequency ν_1, and to the ionization continuum by absorption of another photon with the same frequency ν_1. Once having obtained the 1cR2PI-TOF mass spectrum of the selected species at the resonance frequency ν_1, the intensity of the laser emitting at ν_1 is lowered so as to reduce the TOF ion pattern to less than 10%. Then, by superimposing a second laser of variable frequency ν_2, which alone does not produce any significant signal in the spectral region of interest, there is a pronounced increase in the intensity of the TOF signal of a characteristic ion only when the 2cR2PI process takes place. The value of ν_2 corresponding to the signal onset provides a measure of the ionization threshold of the species.

The energetics involved in diastereomeric **Rr** or **Rs** is determined as follows: The dissociation energy D_0'' of ground-state **Rr** is computed from Equation (1), namely, from the difference between its dissociative ionization threshold ($h\nu_1[\mathbf{Rr}^*] + h\nu_2[\mathbf{R}^+ + \mathbf{r}]$; Figure 1) and the ionization threshold of bare **R** ($\mathrm{IP}(\mathbf{R}) = h\nu_1[\mathbf{R}^*] + h\nu_2[\mathbf{R}^+]$). The dissociation energy D_0^+ of ionic cluster $\mathbf{Rr}^+$ is calculated from Equation (2), namely, from the difference between its dissociative ionization threshold ($h\nu_1[\mathbf{Rr}^*] + h\nu_2[\mathbf{R}^+ + \mathbf{r}]$; Figure 1) and its

[*] Prof. M. Speranza
Facoltà di Farmacia, Dipartimento No. 64
(Chimica e Tecnologia delle Sostanze Biologicamente Attive)
Università di Roma "La Sapienza"
P.le A. Moro 5, I-00185 Rome (Italy)
Fax: (+39) 6-49913602
E-mail: speranza@axrma.uniroma1.it
Dr. A. Latini, Dr. D. Toja, Prof. A. Giardini-Guidoni
Dipartimento di Chimica, Università di Roma "La Sapienza"
Rome (Italy)
Dr. S. Piccirillo
Dipartimento di Scienze e Tecnologie Chimiche
Università di Roma "Tor Vergata", Rome (Italy)

[**] This work was supported by the Ministero della Università e della Ricerca Scientifica e Tecnologica (MURST) and the Consiglio Nazionale delle Ricerche (CNR). The help and advice from Professor F. Cacace are gratefully acknowledged.

  1433-7851/99/3806-0815 $ 17.50+.50/0